European Heart Journal (2007) **28**, 613–627
doi:10.1093/eurheartj/ehl365

Molecular signature of recovery following combination left ventricular assist device (LVAD) support and pharmacologic therapy

Jennifer L. Hall[1]*, Emma J. Birks[2,3], Suzanne Grindle[1], Martin E. Cullen[2], Paul J. Barton[2], James E. Rider[1], Sangjin Lee[1], Subash Harwalker[1], Ami Mariash[1], Neeta Adhikari[1], Nathan J. Charles[1], Leanne E. Felkin[2], Sean Polster[1], Robert S. George[2], Leslie W. Miller[1], and Magdi H. Yacoub[2,4]

[1] *Lillehei Heart Institute, Division of Cardiology, Department of Medicine, University of Minnesota, Mayo Mail Code 508, 420 Delaware Street SE, Minneapolis, MN 55455, USA;* [2] *Heart Science Centre, National Heart and Lung Institute, Imperial College, Harefield, Middlesex, UK;* [3] *Transplant Unit, Royal Brompton and Harefield NHS Trust, Harefield, Middlesex, UK; and* [4] *University of Florence, Florence, Italy*

Received 9 July 2006; revised 29 September 2006; accepted 20 October 2006; online publish-ahead-of-print 28 November 2006

See page 522 for the editorial comment on this article (doi:10.1093/eurheartj/ehl555)

KEYWORDS
Heart failure;
Left ventricular assist device;
EPAC2;
Genomics;
Gene expression

Aims A novel combination therapy consisting of a left ventricular assist device (LVAD) combined with pharmacologic therapy including the selective β_2-agonist, clenbuterol, has shown promise in restoring ventricular function in patients with heart failure. The aim of this study was to identify common genes and signalling pathways whose expression was associated with reversal of heart failure and restoration of ventricular function.
Methods and results Microarray analysis was performed on six paired human heart samples harvested at the time of LVAD implant and at the time of LVAD explant for recovery of ventricular function (post). Follow-up data shows that the improvements in ventricular function have been maintained for an average of 3.8 years post-explant. Analysis of the gene expression data revealed: (i) a significant association of integrin pathway signalling with recovery and (ii) the identification of several novel targets including, EPAC2, in the well-described cAMP pathway whose expression was down-regulated with recovery, and was associated with improvements in cardiac contractility, metabolism, and function.
Conclusion This data set represents the first description of signalling pathways associated with the functional recovery of end-stage human heart failure and the identification of new targets in the human heart that are modified by this combination therapy.

Introduction

Heart failure is a syndrome of increasing prevalence resulting in high mortality and enormous economic impact.[1] Progression to heart failure involves progressive remodelling of the ventricle characterized by structural changes and changes in expression of a multitude of genes.

The current limitations of animal models to replicate a complex disease such as heart failure are becoming more apparent. The use of human tissue to define critical gene and signalling pathways governing cardiovascular remodelling is thus of utmost importance. The ability to analyse paired human heart samples from patients in end-stage heart failure pre- and post-left ventricular assist device (LVAD) has been useful in identifying genes that are involved in reverse remodelling of the dilated heart.[2–11] However, although partial recovery of myocyte function has been reported with the LVAD,[12–14] only 5% of these patients achieve sufficient recovery of function to allow explant of the device.[15] A novel combination therapy consisting of unloading of the ventricle with an LVAD followed by an initiation of five drugs designed to induce myocardial reverse remodelling plus a selective β_2-agonist, clenbuterol, has shown promise in near total recovery and maintaining function in patients with non-ischaemic refractory heart failure.[16,17] To our knowledge, this is the first study to identify changes in gene expression, including expression of components of signalling pathways that occur in the functional recovery of end-stage human heart failure.

Methods

Patients

A total of 15 patients were prospectively recruited into a study in which they received combination therapy (further details of recruitment are provided in Birks *et al.*, NEJM).[18] Of these 15 patients, 11

* Corresponding author. Tel: +1 612 626 4566; fax: +1 612 626 4411.
E-mail address: jlhall@umn.edu

recovered sufficiently to be explanted. The array analysis was performed on six patients with non-ischaemic cardiomyopathy in which sufficient tissue was harvested. All six received the combination therapy that initially included placement of an LVAD. Early post-operatively, all patients received β-blockers, an ACE-inhibitor, an angiotensin II blocker, digoxin, and an aldosterone receptor-blocker at 2–3 months, which was followed by the addition of the β_2-agonist clenbuterol. Mean ejection fraction (EF) at implantation was 8.5 ± 3.5% (*Table 1*). Immediately prior to explantation, mean EF, with the pump turned off for 15 min, was 65.8%. Myocardial left ventricular samples were collected during both LVAD implantation and explantation. All tissues were immediately frozen in liquid nitrogen and stored at −80°C. The Royal Brompton and Harefield NHS Trust Ethics Committee and the University of Minnesota Institutional Review Board approved the study and informed consent was obtained from all participating patients prior to tissue collection.

Sample preparation

Tissue collection, RNA isolation, cDNA synthesis, *in vitro* transcription-synthesis of biotin-labelled cRNA, target hybridization, and probe array was performed as previously described.[5]

Real-time quantitative PCR

Real-time quantitative PCR (RTQPCR) was used in both collaborating laboratories as previously described at the University of Minnesota with the Roche Light Cycler,[5] and Imperial College London with Taqman (Applied Biosystems).[3] Primers included:

integrin α5 Forward 5′-AGCCTCAGAAGGAGGAGGAC-3′
integrin α5 Reverse 5′-GGTTAATGGGGTGATTGGTG-3′
α1 actinin Forward 5′-TCATCTCAGGTGAACGCTTG-3′
α1 actinin Reverse 5′-AGATGTCCTGGATGGCAAAG-3′
GAPDH Forward 5′-ACCACAGTCCATGCCATCAC-3′
GAPDH Reverse 5′-TCCACCACCCTGTTGCTGTA-3′.

Transcripts analysed at Imperial College London using Applied Biosystems' Assays on Demand included Sfrp1 (Hs00610060_m1), AGAT (Hs00155208_m1), and Rap guanine nucleotide exchange factor (RAPGEF4/EPAC2) (Hs00199754_m1).

Data analysis

To define the signalling pathways highly enriched with genes whose expression was significant in the recovering hearts, we utilized Ingenuity Pathways Analysis (www.ingenuity.com). Ingenuity is one of several commercially available programs that dynamically computes a large 'global' molecular network based on hundreds of thousands of curated direct and indirect physical and functional interactions between orthologous mammalian genes from the published, peer-reviewed content in Ingenuity's Knowledge Base. This allowed us to test whether relationships existed between the list of statistically significant genes generated from analysing paired pre- and post-LVAD samples from a cohort of recovered patients. The Ingenuity Pathways Knowledge Base currently contains well over 1 000 000 expert modeled findings plus several hundreds of thousands of additional interactions acquired by automated extraction processes. Significance/*P*-values in Ingenuity Pathways Analysis are calculated based on a hypergeometric distribution calculated via the computationally efficient Fisher's Exact Test for 2×2 contingency tables. More precisely, it is the right-tailed Fisher's Exact test given that only over-represented functional pathway annotations are listed. Two gene lists were imported into Ingenuity for the analysis. The first was a paired *T*-test of pre- vs. post-LVAD samples with a *P*-value < 0.05 with no cutoff for fold change (515 genes). The second list was generated from a paired *T*-test with a more stringent set of parameters—*P*-value < 0.01 (263 genes) (*Table 2*). The final analysis included the intersection of genes that were significant at $P < 0.01$ with both paired and unpaired *T*-tests to generate the list of 98 genes in *Table 3*. This type of analysis enriches genes that are consistently expressed in all pre- and post-LVAD samples and genes that are reproducible either up- or down-regulated following LVAD explant.

Table 1 Patient data from six patients achieving recovery from combination therapy. Table includes age at the time of LVAD implant, gender, EF pre-implant and pre-explant, inotropes, and time on LVAD (days). DP, dopamine; DB, dobutamine; NA, noradrenaline; ML, milrinone

Age	Sex	EF (%) pre-implant	EF (%) pre-explant	Inotropes	Days of LVAD support
49	M	5	45	DP/DB	384
33	F	10	66	DB	503
35	M	7	71	DP/NA	388
53	M	14	72	DP/ML	577
41	M	10	60	DP	156
44	M	5	60	DP/DB	185

Results

Table 1 outlines the patient data. These six patients are now a mean of 3.8 (range 2–4.7) years post-explantation and have successfully maintained the initial improvements in cardiac function seen with this combination therapy. The objective of this study was to begin to define key genes and signalling pathways that were associated with recovery from human heart failure. We outline a series of three different analyses that (i) identify pathways significantly enriched with genes whose expression is statistically different between heart failure and recovery, (ii) reveal novel genes in a well-described pathway known to play an important role in cardiovascular function (cAMP signalling), and (iii) determine interaction/cross talk among pathways of interest by focusing on new gene targets.

A total of 263 genes were identified as significantly up- or down-regulated in the recovered hearts (paired *T*-test, $P < 0.01$) (*Table 2*). The intersection of genes that were statistically significant using both as paired and unpaired *T*-test were also identified (98 genes, $P < 0.01$, *Table 3*). This intersection approach produces a list of genes with relatively low variability at baseline and which are consistently modulated in response to the recovery therapy. This approach allows us to identify and focus on particular genes of interest for further analysis—akin to the *modus operandi* of many classically trained biologists.

An alternative approach is to examine the profile of genes together as a whole with the goal of identifying networks that are altered in the process of recovery from heart failure. To do this we used Ingenuity, one of several commercially available programs that construct connectivity networks of genes curated from the literature. Put simply, one imports gene lists into the Ingenuity database and the program overlays these genes into several described networks to identify the best overall fit. In order to optimize the use of all genes in the signalling networks, we utilized Ingenuity's Pathways Analysis program, which employed a right-tailed Fisher's exact test. One of the most significant pathways identified was the integrin pathway with a *P*-value of 0.006. Genes in the integrin signalling pathway included integrin α5 (ITGA5, up-regulated 2.0-fold), α1

Table 2 List of 263 genes significantly changed with a paired *T*-test following recovery in six patients receiving combination therapy [$P < 0.01$, $n =$ six paired samples (pre-LVAD implant, post-LVAD, post-explant)]

Gene name	Gene description	Gene symbol	Fold change
	Up-regulated in explant		
202212_at	pescadillo homolog 1, containing BRCT domain	PES1	5.019000053
221973_at	CDNA clone IMAGE:5217021		4.764999866
206638_at	5-hydroxytryptamine (serotonin) receptor 2B	HTR2B	4.355000019
213993_at	spondin 1, extracellular matrix protein	SPON1	4.354000092
219896_at	dopamine receptor D1 interacting protein	DRD1IP	4.295000076
203699_s_at	Deiodinase, iodothyronine, type II	DIO2	3.625
218028_at	elongation of very long chain fatty acids (FEN1/Elo2, SUR4/Elo3, yeast)-like 1	ELOVL1	3.49000001
215886_x_at	ubiquitin specific protease 12	USP12	3.375
220789_s_at	transforming growth factor beta regulator 4	TBRG4	3.059000015
210683_at	Neurturin	NRTN	2.905999899
204934_s_at	hepsin (transmembrane protease, serine 1)	HPN	2.898999929
208262_x_at	Mediterranean fever	MEFV	2.892999887
203828_s_at	natural killer cell transcript 4	NK4	2.734999895
220981_x_at	nuclear RNA export factor 2	NXF2	2.673000097
219530_at	hypothetical protein FLJ21816	FLJ21816	2.661000013
201389_at	integrin, alpha 5 (fibronectin receptor, alpha polypeptide)	ITGA5	2.54399991
65086_at	hypothetical protein MGC3262	MGC3262	2.217999935
222234_s_at	hypothetical protein MGC3101	MGC3101	2.217000008
210968_s_at	reticulon 4	RTN4	2.157000065
213473_at	BRCA1 associated protein	BRAP	1.985999942
211160_x_at	actinin, alpha 1	ACTN1	1.98300004
216975_x_at	neuronal PAS domain protein 1	NPAS1	1.970000029
209280_at	mannose receptor, C type 2	MRC2	1.953999996
219594_at	ninjurin 2	NINJ2	1.934000015
203927_at	nuclear factor of kappa light polypeptide gene enhancer in B-cells inhibitor, epsilon	NFKBIE	1.932000041
213119_at	solute carrier family 36 (proton/amino acid symporter), member 1	SLC36A1	1.90199995
209122_at	adipose differentiation-related protein	ADFP	1.899000049
216009_at	solute carrier family 39 (zinc transporter), member 9	SLC39A9	1.886999965
221653_x_at	apolipoprotein L, 2	APOL2	1.886999965
219847_at	histone deacetylase 11	HDAC11	1.868999958
206397_x_at	growth differentiation factor 1	GDF1	1.845000029
206332_s_at	interferon, gamma-inducible protein 16	IFI16	1.835000038
218388_at	6-phosphogluconolactonase	PGLS	1.812000036
213527_s_at	similar to hypothetical protein MGC13138	LOC146542	1.812000036
219602_s_at	family with sequence similarity 38, member B	FAM38B	1.81099999
214752_x_at	filamin A, alpha (actin binding protein 280)	FLNA	1.741999984
221889_at	potassium channel tetramerization domain containing 13	KCTD13	1.735000014
220668_s_at	DNA (cytosine-5-)-methyltransferase 3 beta	DNMT3B	1.730000019
205441_at	hypothetical protein FLJ22709	FLJ22709	1.726999998
212668_at	E3 ubiquitin ligase SMURF1	SMURF1	1.725999951
212680_x_at	LIM domain kinase 2	LIMK2	1.718999982
216685_s_at	methylthioadenosine phosphorylase	MTAP	1.715999961
210931_at	ring finger protein (C3H2C3 type) 6	RNF6	1.67900002
212466_at	sprouty-related, EVH1 domain containing 2	SPRED2	1.672999978
220518_at	target of Nesh-SH3	TARSH	1.664000034
205098_at	chemokine (C-C motif) receptor 1	CCR1	1.661999941
212766_s_at	hypothetical protein FLJ12671	FLJ12671	1.659999967
207542_s_at	aquaporin 1 (channel-forming integral protein, 28 kDa)	AQP1	1.657999992
212525_s_at	H2A histone family, member X	H2AFX	1.646000028
208871_at	dentatorubral-pallidoluysian atrophy (atrophin-1)	DRPLA	1.639000058
215175_at	pecanex homolog (Drosophila)	PCNX	1.626000047
220081_x_at	hydroxysteroid (17-beta) dehydrogenase 7	HSD17B7	1.621999979
202096_s_at	benzodiazapine receptor (peripheral)	BZRP	1.600999951
217668_at	small nuclear ribonucleoprotein D3 polypeptide 18 kDa	SNRPD3	1.600999951
201315_x_at	interferon induced transmembrane protein 3 (1-8U)	IFITM3	1.593000054
218055_s_at	WD repeat domain 41	WDR41	1.592000008
204931_at	transcription factor 21	TCF21	1.588999987
200621_at	cysteine and glycine-rich protein 1	CSRP1	1.588000059
203882_at	interferon-stimulated transcription factor 3, gamma 48 kDa	ISGF3G	1.565999985

Continued

Table 2 *Continued*

Gene name	Gene description	Gene symbol	Fold change
202856_s_at	solute carrier family 16 (monocarboxylic acid transporters), member 3	SLC16A3	1.552000046
202274_at	actin, gamma 2, smooth muscle, enteric	ACTG2	1.546000004
212843_at	neural cell adhesion molecule 1	NCAM1	1.539000034
212300_at	taxilin	DKFZp451J0118	1.536000013
38487_at	stabilin 1	STAB1	1.534999967
218248_at	FLJ22794 protein	FLJ22794	1.532999992
207988_s_at	actin related protein 2/3 complex, subunit 2, 34kDa	ARPC2	1.524999976
202692_s_at	upstream binding transcription factor, RNA polymerase I	UBTF	1.506999969
200634_at	profilin 1	PFN1	1.506000042
205824_at	heat shock 27 kDa protein 2	HSPB2	1.501999974
216165_at	CDNA: FLJ21997 fis, clone HEP06590		1.488000035
213422_s_at	hypothetical protein MGC3047	MGC3047	1.481999993
205508_at	sodium channel, voltage-gated, type I, beta	SCN1B	1.480999947
52651_at	collagen, type VIII, alpha 2	COL8A2	1.470000029
213867_x_at	actin, beta	ACTB	1.460000038
212775_at	KIAA0657 protein	KIAA0657	1.458999991
222055_at	CGI-105 protein	CGI-105	1.458999991
220208_at	a disintegrin-like and metalloprotease (reprolysin type) with thrombospondin type 1 motif, 13	ADAMTS13	1.450000048
200872_at	S100 calcium binding protein A10 (annexin II ligand, calpactin I, light polypeptide (p11))	S100A10	1.450000048
209042_s_at	ubiquitin-conjugating enzyme E2G 2 (UBC7 homolog, yeast)	UBE2G2	1.447000027
209454_s_at	TEA domain family member 3	TEAD3	1.43599999
202621_at	interferon regulatory factor 3	IRF3	1.432999969
220924_s_at	solute carrier family 38, member 2	SLC38A2	1.429999948
200801_x_at	actin, beta	ACTB	1.42900002
210113_s_at	NACHT, leucine rich repeat and PYD containing 1	NALP1	1.427000046
208610_s_at	serine/arginine repetitive matrix 2	SRRM2	1.424000025
221794_at	dedicator of cytokinesis 6	DOCK6	1.419999957
214924_s_at	OGT(O-Glc-NAc transferase)-interacting protein 106 kDa	OIP106	1.407999992
209426_s_at	alpha-methylacyl-CoA racemase	AMACR	1.404999971
220319_s_at	myosin regulatory light chain interacting protein	MYLIP	1.401000023
209810_at	surfactant, pulmonary-associated protein B	SFTPB	1.39199996
208944_at	transforming growth factor, beta receptor II (70/80 kDa)	TGFBR2	1.39199996
202203_s_at	autocrine motility factor receptor	AMFR	1.383000016
214107_x_at	Similar to aminopeptidase puromycin sensitive; puromycin-sensitive aminopeptidase; metalloproteinase MP100 (LOC390819), mRNA		1.368999958
200848_at	S-adenosylhomocysteine hydrolase-like 1	AHCYL1	1.36500001
218574_s_at	LIM and cysteine-rich domains 1	LMCD1	1.358999968
202725_at	polymerase[35] II (DNA directed) polypeptide A, 220 kDa	POLR2A	1.342000008
221564_at	HMT1 hnRNP methyltransferase-like 1 (S. cerevisiae)	HRMT1L1	1.337000012
211271_x_at	polypyrimidine tract binding protein 1	PTBP1	1.337000012
218041_x_at	solute carrier family 38, member 2	SLC38A2	1.335999966
203818_s_at	splicing factor 3a, subunit 3, 60 kDa	SF3A3	1.335000038
202440_s_at	suppression of tumorigenicity 5	ST5	1.332999945
200044_at	splicing factor, arginine/serine-rich 9	SFRS9	1.327999949
205097_at	solute carrier family 26 (sulfate transporter), member 2	SLC26A2	1.322000027
208625_s_at	eukaryotic translation initiation factor 4 gamma, 1	EIF4G1	1.315000057
219314_s_at	zinc finger protein 219	ZNF219	1.31099999
200677_at	pituitary tumor-transforming 1 interacting protein	PTTG1IP	1.309999943
204115_at	guanine nucleotide binding protein (G protein), gamma 11	GNG11	1.294999957
37872_at	jerky homolog (mouse)	JRK	1.29400003
219377_at	chromosome 18 open reading frame 11	C18orf11	1.287999988
211251_x_at	nuclear transcription factor Y, gamma	NFYC	1.281000018
211765_x_at	peptidylprolyl isomerase A (cyclophilin A)	PPIA	1.279000044
201125_s_at	integrin, beta 5	ITGB5	1.26699996
217717_s_at	tyrosine 3-monooxygenase/tryptophan 5-monooxygenase activation protein, beta polypeptide	YWHAB	1.261000037
200964_at	ubiquitin-activating enzyme E1 (A1S9T and BN75 temperature sensitivity complementing)	UBE1	1.258000016
205526_s_at	katanin p60 (ATPase-containing) subunit A 1	KATNA1	1.241000056
201692_at	opioid receptor, sigma 1	OPRS1	1.233999968
217943_s_at	hypothetical protein FLJ10350	FLJ10350	1.233999968

Continued

Table 2 *Continued*

Gene name	Gene description	Gene symbol	Fold change
208012_x_at	SP110 nuclear body protein	SP110	1.228999972
203605_at	signal recognition particle 54 kDa	SRP54	1.19599998
211761_s_at	Siah-interacting protein	SIP	1.184999943
212886_at	DKFZP434C171 protein	DKFZP434C171	1.175999999
203857_s_at	for protein disulfide isomerase-related	PDIR	1.174000025
209134_s_at	ribosomal protein S6	RPS6	1.171000004
56197_at	phospholipid scramblase 3	PLSCR3	1.156999946
	Down-regulated in explant		
215047_at	BIA2	BIA2	5.55700016
207175_at	adipocyte, C1Q and collagen domain containing	ACDC	5.040999889
221583_s_at	potassium large conductance calcium-activated channel, subfamily M, alpha member 1	KCNMA1	3.854000092
221244_s_at	3-phosphoinositide dependent protein kinase-1	PDPK1	3.700000048
214858_at	Clone 24566 mRNA sequence		3.645999908
210911_at	inhibitor of DNA binding 2, dominant negative helix-loop-helix protein	ID2	3.309000015
213844_at	homeo box A5	HOXA5	2.993000031
204962_s_at	centromere protein A, 17 kDa	CENPA	2.944999933
203178_at	arginine:glycine amidinotransferase	AGAT	2.858999968
216733_s_at	arginine:glycine amidinotransferase	AGAT	2.849999905
219934_s_at	sulfotransferase family 1E, estrogen-preferring, member 1	SULT1E1	2.802000046
204317_at	G-2 and S-phase expressed 1	GTSE1	2.691999912
215335_at	MRNA; cDNA DKFZp434M0835 (from clone DKFZp434M0835)		2.65199995
205041_s_at	orosomucoid 1	ORM1	2.650000095
211923_s_at	zinc finger protein 471	ZNF471	2.604000092
208427_s_at	ELAV (embryonic lethal, abnormal vision, Drosophila)-like 2 (Hu antigen B)	ELAVL2	2.595999956
215512_at	similar to S. cerevisiae SSM4	TEB4	2.555000067
202036_s_at	secreted frizzled-related protein 1	SFRP1	2.365999937
215058_at	hypothetical protein MGC24039	MGC24039	2.364000082
202037_s_at	secreted frizzled-related protein 1	SFRP1	2.247999907
204111_at	histamine N-methyltransferase	HNMT	2.154000044
204401_at	potassium intermediate/small conductance calcium-activated channel, subfamily N, member 4	KCNN4	2.092999935
208084_at	integrin, beta 6	ITGB6	2.078000069
210440_s_at	CDC14 cell division cycle 14 homolog A (S. cerevisiae)	CDC14A	2.03399992
200635_s_at	protein tyrosine phosphatase, receptor type, F	PTPRF	2.025000095
211553_x_at	apoptotic protease activating factor	APAF1	2.019999981
216539_at	similar to homologue of MJD, high homology to a genomic sequence in Xp22	LOC92552	2.015000105
220523_at	hypothetical protein FLJ22843	FLJ22843	2.009000063
207342_at	cyclic nucleotide gated channel beta 1	CNGB1	1.995000005
204328_at	epidermodysplasia verruciformis 1	EVER1	1.962000012
205856_at	solute carrier family 14 (urea transporter), member 1 (Kidd blood group)	SLC14A1	1.940999985
220068_at	pre-B lymphocyte gene 3	VPREB3	1.934999943
210821_x_at	centromere protein A, 17kDa	CENPA	1.907999992
210280_at	myelin protein zero (Charcot-Marie-Tooth neuropathy 1B)	MPZ	1.894000053
207154_at	deiodinase, iodothyronine, type III	DIO3	1.824000001
211734_s_at	Fc fragment of IgE, high affinity I, receptor for; alpha polypeptide	FCER1A	1.796000004
221202_at	gb:NM_018523.1 /DB_XREF = gi:8924154 /GEN = PRO2325 /FEA = FLmRNA /CNT=2 /TID = Hs.31535.0 /TIER = FL /STK=0 /UG = Hs.31535 /LL = 55393 /DEF = Homo sapiens hypothetical protein PRO2325 (PRO2325), mRNA. /PROD = hypoth		1.779000044
209008_x_at	keratin 8	KRT8	1.771000028
204094_s_at	KIAA0669 gene product	KIAA0669	1.766000032
217790_s_at	signal sequence receptor, gamma (translocon-associated protein gamma)	SSR3	1.753999949
200730_s_at	protein tyrosine phosphatase type IVA, member 1	PTP4A1	1.697000027
221196_x_at	c6.1A	C6.1A	1.694000006

Continued

Table 2 *Continued*

Gene name	Gene description	Gene symbol	Fold change
201297_s_at	MOB1, Mps One Binder kinase activator-like 1B (yeast)	MOBK1B	1.684000015
206959_s_at	UPF3 regulator of nonsense transcripts homolog A (yeast)	UPF3A	1.672999978
211138_s_at	kynurenine 3-monooxygenase (kynurenine 3-hydroxylase)	KMO	1.669999957
204992_s_at	profilin 2	PFN2	1.664999962
201433_s_at	phosphatidylserine synthase 1	PTDSS1	1.664000034
214567_s_at	chemokine (C motif) ligand 1	XCL1	1.662999988
206361_at	G protein-coupled receptor 44	GPR44	1.659000039
208563_x_at	POU domain, class 3, transcription factor 3	POU3F3	1.654000044
203858_s_at	COX10 homolog, cytochrome c oxidase assembly protein, heme A: farnesyltransferase (yeast)	COX10	1.646000028
221465_at	gb:NM_003696.1 /DB_XREF = gi:4505520 /GEN = OR6A1 /FEA = FLmRNA /CNT=2 /TID = Hs.248186.0 /TIER = FL /STK=0 /UG = Hs.248186 /LL = 8590 /DEF = Homo sapiens olfactory receptor, family 6, subfamily A, member 1 (OR6A1)		1.644999981
216667_at	ribonuclease, RNase A family, 2 (liver, eosinophil-derived neurotoxin)	RNASE2	1.633000016
204464_s_at	endothelin receptor type A	EDNRA	1.618999958
214056_at	myeloid cell leukemia sequence 1 (BCL2-related)	MCL1	1.600999951
200733_s_at	protein tyrosine phosphatase type IVA, member 1	PTP4A1	1.593000054
216753_at	gb:AK025152.1 /DB_XREF = gi:10437612 /FEA = mRNA /CNT=1 /TID = Hs.306773.0 /TIER = ConsEnd /STK=0 /UG = Hs.306773 /UG_TITLE = Homo sapiens cDNA: FLJ21499 fis, clone COL05634 /DEF = Homo sapiens cDNA: FLJ21499 fis		1.588999987
214919_s_at	eukaryotic translation initiation factor 4E binding protein 3 [BLAST]	EIF4EBP3	1.588999987
217967_s_at	chromosome 1 open reading frame 24	C1orf24	1.583999991
203870_at	ubiquitin specific protease 46	USP46	1.562999964
202358_s_at	sorting nexin 19	SNX19	1.557000041
203917_at	coxsackie virus and adenovirus receptor	CXADR	1.542999983
208846_s_at	voltage-dependent anion channel 3	VDAC3	1.542000055
210175_at	chromosome 2 open reading frame 3	C2orf3	1.539999962
201211_s_at	DEAD (Asp-Glu-Ala-Asp) box polypeptide 3, X-linked	DDX3X	1.536000013
206272_at	CDNA clone MGC:88280 IMAGE:30320725, complete cds [BLAST]		1.532999992
209442_x_at	ankyrin 3, node of Ranvier (ankyrin G)	ANK3	1.531999946
212528_at	Clone IMAGE:3605655, Mrna		1.527999997
221523_s_at	Ras-related GTP binding D	RRAGD	1.524000049
206978_at	Transcribed sequences		1.518000007
212253_x_at	dystonin	DST	1.514000058
212243_at	glutamate receptor, ionotropic, N-methyl D-aspartate-like 1A	GRINL1A	1.508999944
216531_at	YY2 transcription factor	YY2	1.506999969
200931_s_at	vinculin	VCL	1.504999995
213178_s_at	mitogen-activated protein kinase 8 interacting protein 3	MAPK8IP3	1.501999974
208769_at	eukaryotic translation initiation factor 4E binding protein 2	EIF4EBP2	1.495000005
212214_at	optic atrophy 1 (autosomal dominant)	OPA1	1.491000056
207066_at	histidine rich calcium binding protein	HRC	1.49000001
214558_at	G protein-coupled receptor 12	GPR12	1.485000014
214835_s_at	succinate-CoA ligase, GDP-forming, beta subunit	SUCLG2	1.472000003
214053_at	CDNA FLJ44318 fis, clone TRACH3000780		1.468000054
203864_s_at	actinin, alpha 2	ACTN2	1.467000008
221405_at	gb:NM_016317.1 /DB_XREF = gi:7705928 /GEN = LOC51190 /FEA = FLmRNA /CNT = 2 /TID = Hs.278964.0 /TIER = FL /STK = 0 /UG = Hs.278964 /LL = 51190 /DEF = Homo sapiens neutral sphingomyelinase (LOC51190), mRNA. /PROD = neutra		1.460999966
214582_at	phosphodiesterase 3B, cGMP-inhibited	PDE3B	1.452000022
203284_s_at	heparan sulfate 2-O-sulfotransferase 1	HS2ST1	1.44599998
210236_at	protein tyrosine phosphatase, receptor type, f polypeptide (PTPRF), interacting protein (liprin), alpha 1	PPFIA1	1.445000052
221533_at	growth and transformation-dependent protein	E2IG5	1.437999964
202263_at	NAD(P)H:quinone oxidoreductase type 3, polypeptide A2	NQO3A2	1.432999969
220239_at	kelch-like 7 (Drosophila)	KLHL7	1.427999973
208936_x_at	lectin, galactoside-binding, soluble, 8 (galectin 8)	LGALS8	1.424999952
203118_at	proprotein convertase subtilisin/kexin type 7	PCSK7	1.419999957
218549_s_at	CGI-90 protein	CGI-90	1.411000013

Continued

Table 2 *Continued*

Gene name	Gene description	Gene symbol	Fold change
200862_at	24-dehydrocholesterol reductase	DHCR24	1.409999967
204675_at	steroid-5-alpha-reductase, alpha polypeptide 1 (3-oxo-5 alpha-steroid delta 4-dehydrogenase alpha 1)	SRD5A1	1.409000039
216349_at	fumarate hydratase	FH	1.404000044
219065_s_at	C21orf19-like	CGI-27	1.399000049
203559_s_at	amiloride binding protein 1 (amine oxidase (copper-containing))	ABP1	1.398000002
213465_s_at	protein phosphatase 1, regulatory subunit 7	PPP1R7	1.396000028
219647_at	popeye domain containing 2	POPDC2	1.389000058
215918_s_at	spectrin, beta, non-erythrocytic 1	SPTBN1	1.378000021
214508_x_at	cAMP responsive element modulator	CREM	1.370000005
203084_at	transforming growth factor, beta 1 (Camurati-Engelmann disease)	TGFB1	1.36500001
219499_at	Sec61 alpha 2 subunit (*S. cerevisiae*)	SEC61A2	1.35800004
212461_at	ornithine decarboxylase antizyme inhibitor	OAZIN	1.353999972
213253_at	SMC2 structural maintenance of chromosomes 2-like 1 (yeast)	SMC2L1	1.353000045
203861_s_at	actinin, alpha 2	ACTN2	1.345000029
212845_at	sterile alpha motif domain containing 4	SAMD4	1.343999982
213148_at	Clone 23568, 23621, 23795, 23873 and 23874 mRNA sequences		1.325000048
211994_at	protein kinase, lysine deficient 1	PRKWNK1	1.31400001
213567_at	CDNA clone IMAGE:6503168, partial cds		1.312999964
219958_at	chromosome 20 open reading frame 46	C20orf46	1.312000036
201568_at	low molecular mass ubiquinone-binding protein (9.5 kD)	QP-C	1.31099999
202336_s_at	peptidylglycine alpha-amidating monooxygenase	PAM	1.309000015
221894_at	aarF domain containing kinase 2	ADCK2	1.30400002
205512_s_at	programmed cell death 8 (apoptosis-inducing factor)	PDCD8	1.30400002
78330_at	zinc finger protein 335	ZNF335	1.302999973
204042_at	WAS protein family, member 3	WASF3	1.297000051
221502_at	karyopherin alpha 3 (importin alpha 4)	KPNA3	1.292999983
221720_s_at	gb:L11573.1 /DB_XREF = gi:1220354 /FEA = FLmRNA /CNT=1 /TID = HsAffx.900439.1129 /TIER = FL /STK=0 /DEF = Human surfactant protein B mRNA, complete cds. /PROD = 33.1 kDa protein /FL = gb:L11573.1		1.292000055
205303_at	potassium inwardly-rectifying channel, subfamily J, member 8	KCNJ8	1.287999988
214218_s_at	Transcribed sequences		1.279999971
222132_s_at	hypothetical protein FLJ10842	FLJ10842	1.271999955
218003_s_at	FK506 binding protein 3, 25 kDa	FKBP3	1.268000007
217140_s_at	voltage-dependent anion channel 1	VDAC1	1.248999953
217200_x_at	cytochrome b-561	CYB561	1.243999958
202665_s_at	Wiskott-Aldrich syndrome protein interacting protein	WASPIP	1.233999968
217727_x_at	vacuolar protein sorting 35 (yeast)	VPS35	1.23300004
204000_at	guanine nucleotide binding protein (G protein), beta 5	GNB5	1.218999982
219706_at	chromosome 20 open reading frame 29	C20orf29	1.200000048
212595_s_at	DAZ associated protein 2	DAZAP2	1.19599998
206765_at	potassium inwardly-rectifying channel, subfamily J, member 2	KCNJ2	1.190999985
64883_at	motile sperm domain containing 2	MOSPD2	1.190999985
204001_at	small nuclear RNA activating complex, polypeptide 3, 50 kDa	SNAPC3	1.17900002
49329_at	hypothetical protein FLJ14360	FLJ14360	1.171000004
218531_at	hypothetical protein FLJ21749	FLJ21749	1.164999962
200598_s_at	tumor rejection antigen (gp96) 1	TRA1	1.156000018
200790_at	ornithine decarboxylase 1	ODC1	1.141000032
203116_s_at	ferrochelatase (protoporphyria)	FECH	1.139999986
208632_at	ring finger protein 10	RNF10	1.108999968

actinin (ACTN1, up-regulated 2.4-fold), actin-related protein 2/3 complex (ARP2/3, up-regulated 1.6-fold), GTP-binding protein (Cdc42, up-regulated 1.3-fold), Rhodopsin (RHO, down-regulated 1.3-fold), Vinculin (VCL, down-regulated 1.4-fold), protein phosphatase 1 regulatory subunit (MLCP/PP1R12B, up-regulated 1.5-fold), and β actin (ACTB).[19] We have recently published this work in more detail.[19] RTQPCR was used to confirm a subset of these selected genes that fall in different signalling pathways including alpha 1 actinin (ACTN1) (up-regulated 2.3-fold by RTQPCR, 2.0-fold with array)[19] and alpha-5 integrin (ITGA5) (up-regulated 1.8-fold by RTQPCR, 2.5-fold with array)[19].

Next, we utilized Ingenuity to identify a novel gene in a well-described signalling pathway. The cAMP-mediated signalling pathway, a pathway known to play a key role in heart failure was assigned a less significant *P*-value of 0.5 (compared with 0.006 for the Integrin Pathway). The genes in the cAMP-mediated signalling pathway included Rap guanine nucleotide exchange factor 4

Table 3 List of 98 genes that were significantly changed in recovery patients following combination therapy ($P < 0.01$, $n =$ six paired samples (pre-LVAD (implant), post-LVAD (explant))

Gene name	Gene description	Gene symbol	Fold change
	Up-regulated at explant		
202212_at	pescadillo homolog 1	PES1	5.02
221973_at	cDNA clone IMAGE:5217021		4.76
206638_at	5-hydroxytryptamine (serotonin) receptor 2B	HTR2B	4.36
213993_at	spondin 1, extracellular matrix protein	SPON1	4.35
219896_at	dopamine receptor D1 interacting protein	DRD1IP	4.30
203699_s_at	deiodinase, iodothyronine, type II	DIO2	3.63
218028_at	(FEN1/Elo2, SUR4/Elo3, yeast)-like 1	ELOVL1	3.49
220789_s_at	transforming growth factor beta regulator 4	TBRG4	3.06
220981_x_at	nuclear RNA export factor 2	NXF2	2.67
219530_at	hypothetical protein FLJ21816	FLJ21816	2.66
201389_at	integrin, alpha 5	ITGA5	2.54
210968_s_at	reticulon 4	RTN4	2.16
211160_x_at	actinin, alpha 1	ACTN1	1.98
209280_at	mannose receptor, C type 2	MRC2	1.95
213119_at	solute carrier family 36	SLC36A1	1.90
209122_at	adipose differentiation-related protein	ADFP	1.90
214752_x_at	filamin A, alpha (actin binding protein 280)	FLNA	1.74
221889_at	potassium channel tetramerization domain	KCTD13	1.74
220668_s_at	DNA (cytosine-5-)-methyltransferase 3 beta	DNMT3B	1.73
205098_at	chemokine (C-C motif) receptor 1	CCR1	1.66
220081_x_at	hydroxysteroid (17-beta) dehydrogenase 7	HSD17B7	1.62
202096_s_at	benzodiazapine receptor (peripheral)	BZRP	1.60
200621_at	cysteine and glycine-rich protein 1	CSRP1	1.59
203882_at	interferon-stimulated transcription factor 3	ISGF3G	1.57
202856_s_at	solute carrier family 16	SLC16A3	1.55
212843_at	neural cell adhesion molecule 1	NCAM1	1.54
212300_at	Taxilin	DKFZp451J0118	1.54
38487_at	stabilin 1	STAB1	1.53
207988_s_at	actin related protein 2/3 complex, subunit 2, 34 kDa	ARPC2	1.52
213867_x_at	actin, beta	ACTB	1.46
220208_at	A disintegrin-like and metalloprotease	ADAMTS13	1.45
202621_at	interferon regulatory factor 3	IRF3	1.43
221794_at	dedicator of cytokinesis 6	DOCK6	1.42
221564_at	HMT1 hnRNP methyltransferase-like 1	HRMT1L1	1.34
211271_x_at	polypyrimidine tract binding protein 1	PTBP1	1.34
203818_s_at	splicing factor 3a, subunit 3, 60 kDa	SF3A3	1.34
202440_s_at	suppression of tumorigenicity 5	ST5	1.33
200044_at	splicing factor, arginine/serine-rich 9	SFRS9	1.33
37872_at	jerky homolog (mouse)	JRK	1.29
208012_x_at	SP110 nuclear body protein	SP110	1.23
203605_at	signal recognition particle 54 kDa	SRP54	1.20
56197_at	phospholipid scramblase 3	PLSCR3	1.16
	Down-regulated at explant		
215047_at	BIA2	BIA2	5.56
207175_at	adipocyte, C1Q and collagen domain	ACDC	5.04
221583_s_at	potassium conductance calcium-activated channel	KCNMA1	3.85
221244_s_at	3-phosphoinositide dependent protein kinase-1	PDPK1	3.70
214858_at	Clone 24566 mRNA sequence		3.65
210911_at	inhibitor of DNA binding 2	ID2	3.31
213844_at	homeo box A5	HOXA5	2.99
204962_s_at	centromere protein A, 17 kDa	CENPA	2.94
203178_at	arginine:glycine amidinotransferase	AGAT	2.86
216733_s_at	arginine:glycine amidinotransferase	AGAT	2.85
219934_s_at	sulfotransferase family 1E	SULT1E1	2.80
204317_at	G-2 and S-phase expressed 1	GTSE1	2.69
215335_at	mRNA; cDNA DKFZp434M0835		2.65
215512_at	similar to S. cerevisiae SSM4	TEB4	2.56
202036_s_at	secreted frizzled-related protein 1	SFRP1	2.37
202037_s_at	secreted frizzled-related protein 1	SFRP1	2.25
204401_at	potassium conductance calcium-activated channel	KCNN4	2.09
208084_at	integrin, beta 6	ITGB6	2.08

Continued

Table 3 *Continued*

Gene name	Gene description	Gene symbol	Fold change
210440_s_at	CDC14 cell division cycle 14 homolog A	CDC14A	2.03
220523_at	hypothetical protein FLJ22843	FLJ22843	2.01
204328_at	epidermodysplasia verruciformis 1	EVER1	1.96
207154_at	deiodinase, iodothyronine, type III	DIO3	1.82
209008_x_at	keratin 8	KRT8	1.77
217790_s_at	signal sequence receptor, gamma	SSR3	1.75
200730_s_at	protein tyrosine phosphatase type IVA, member 1	PTP4A1	1.70
206959_s_at	UPF3 regulator of nonsense transcripts homolog A	UPF3A	1.67
204992_s_at	profilin 2	PFN2	1.66
201433_s_at	phosphatidylserine synthase 1	PTDSS1	1.66
206361_at	G protein-coupled receptor 44	GPR44	1.66
203858_s_at	COX10 homolog, cytochrome c oxidase	COX10	1.65
204464_s_at	endothelin receptor type A	EDNRA	1.62
200733_s_at	protein tyrosine phosphatase type IVA, member 1	PTP4A1	1.59
214919_s_at	eukaryotic translation initiation factor 4E binding prt	EIF4EBP3	1.59
217967_s_at	chromosome 1 open reading frame 24	C1orf24	1.58
203870_at	ubiquitin specific protease 46	USP46	1.56
206272_at	cDNA clone MGC:88280 IMAGE:30320725		1.53
209442_x_at	ankyrin 3, node of Ranvier (ankyrin G)	ANK3	1.53
221523_s_at	Ras-related GTP binding D	RRAGD	1.52
206978_at	Transcribed sequences		1.52
212243_at	glutamate receptor, ionotropic,	GRINL1A	1.51
213178_s_at	mitogen-activated protein kinase 8 interacting protein	MAPK8IP3	1.50
207066_at	histidine rich calcium binding protein	HRC	1.49
214835_s_at	succinate-CoA ligase, GDP-forming, beta subunit	SUCLG2	1.47
214053_at	cDNA FLJ44318 fis, clone TRACH3000780		1.47
203284_s_at	heparan sulfate 2-O-sulfotransferase 1	HS2ST1	1.45
220239_at	kelch-like 7 (Drosophila)	KLHL7	1.43
208936_x_at	lectin, galactoside-binding, soluble, 8 (galectin 8)	LGALS8	1.42
218549_s_at	CGI-90 protein	CGI-90	1.41
219647_at	popeye domain containing 2	POPDC2	1.39
215918_s_at	spectrin, beta, non-erythrocytic 1	SPTBN1	1.38
212461_at	ornithine decarboxylase antizyme inhibitor	OAZIN	1.35
213567_at	cDNA clone IMAGE:6503168, partial cds		1.31
201568_at	low molecular mass ubiquinone-binding protein	QP-C	1.31
202336_s_at	peptidylglycine alpha-amidating monooxygenase	PAM	1.31
204042_at	WAS protein family, member 3	WASF3	1.30
221502_at	karyopherin alpha 3 (importin alpha 4)	KPNA3	1.29
221720_s_at	Human surfactant protein B mRNA		1.29
217200_x_at	cytochrome b-561	CYB561	1.24
217727_x_at	vacuolar protein sorting 35 (yeast)	VPS35	1.23

(RAPGEF4 (EPAC2), down-regulated 2.2-fold), protein kinase, cAMP-dependent, regulatory, type I alpha (tissue-specific extinguisher 1) (PKAr, down-regulated 1.5-fold), phosphodiesterase 1A (PDE1A, down-regulated 1.5-fold), phosphodiesterase 3B (PDE3B, down-regulated 1.5-fold), and calcineurin A (PPP3CA/PP2B, (up-regulated 1.4-fold) (*Figure 1*). Despite the lack of significance assigned to this pathway, it permitted us to identify an association between a new member of this well known signalling pathway, EPAC2, and recovery from heart failure. The down-regulation of the recently defined EPAC2 gene in the hearts of all six of the recovered patients and three new additional subjects is shown in *Figure 2A*. The down-regulation of EPAC2 did not occur in a set of non-recovered non-ischaemic patients and was thus unique to the recovered cohort as seen in *Figure 2B*.

The final goal was to highlight previously unrecognized interactions between the genes that were significantly regulated in recovered patients. The goal of this type of analysis is to identify novel signal transduction pathways associated with recovery of end-stage heart failure. Genes found to be statistically significant were grouped onto networks based upon Ingenuity Pathways Knowledge Base of interacting genes. Two networks were identified (*Figure 3* and *4*). The first network is shown in *Figure 3*. Of particular interest in this pathway was the link between EPAC2 and insulin. This interaction is supported by a number of recent studies in pancreatic islet cells and may play an important role in metabolism as well as its better known role in calcium signalling. Secondly, a number of the genes included in the integrin signalling in *Figure 1* are shown to interact with TNF (alpha-5 integrin) and c-myc (alpha 1 actinin) in *Figure 3*. The

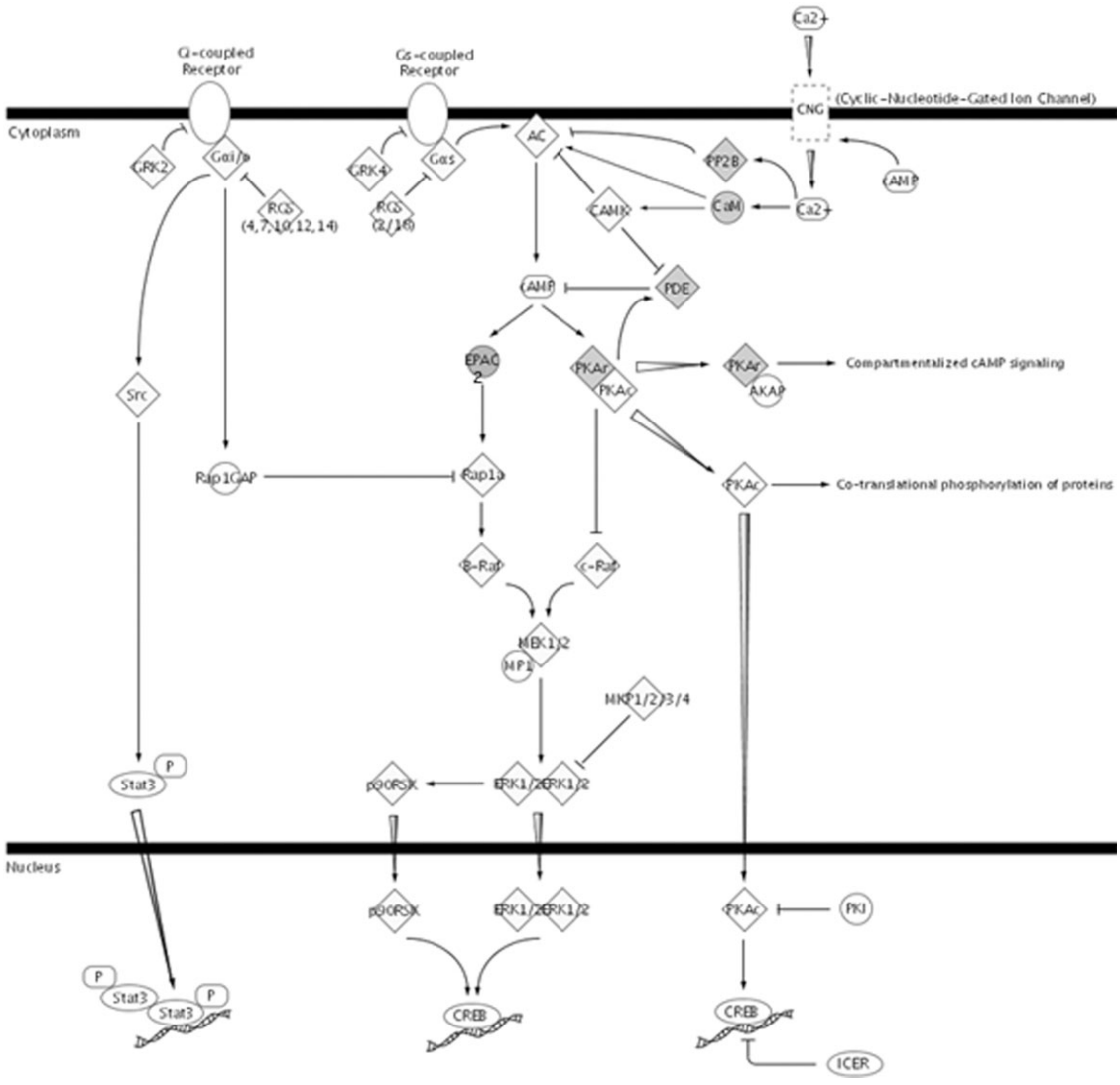

Figure 1 Identification of genes in the well known cAMP-mediated signalling pathway whose expression was altered in association with recovery. Shaded symbols represent genes whose expression was significantly altered in explanted vs. implanted samples. This pathway analysis approach highlighted a previously unacknowledged role for EPAC2 in this process of recovery.

second network identified is shown in *Figure 4* and includes arginine:glycine amidinotransferase (AGAT, GATM) (down-regulated 2.9-fold by array).[20] RTQPCR reconfirmed this finding, and identified a 3.4-fold down-regulation. Interestingly, AGAT, which is an enzyme that regulates expression of creatine, appears to interact with MAPKAP2 and IL-4.

Discussion

To our knowledge, this is the first full report of the signature of genes associated with the recovery of refractory human heart failure. In this analysis, we highlight: (i) a significant association between recovery and integrin signalling pathways and (ii) a significant down-regulation of the novel gene EPAC2, a guanine nucleotide exchange factor that binds to cAMP and is associated with signalling pathways that improve β-adrenergic responsiveness and myocyte contractility. The identification of these networks came about through an integrated approach of both focusing in on single genes and utilizing a systems approach to analyse the data. Although the classical single gene approach has been successful in identifying dysregulated molecular and cellular signalling associated with heart failure, we now have the opportunity to exploit new approaches to further understand the mechanisms of cardiovascular disease and recovery. These new approaches include system-wide approaches including those used in this study in which we are able to organize genes into pathways associated with recovery from end-stage heart failure.

LV unloading in end-stage heart failure patients with LVAD support has been shown to improve myocardial structure and function, including improving β-adrenergic responsiveness and myocyte contractility.[21,22] Several working groups, including our own, have defined changes in gene expression that occur with LVAD support that appear to be important in improving β-adrenergic responsiveness and calcium handling including partial restoration of β-receptor density, and altered regulation of the genes in G-protein-regulated signalling and calcium handling.[4,5,7,23,24] However, despite near normalization of these measurements, these patients rarely achieve sufficient recovery of

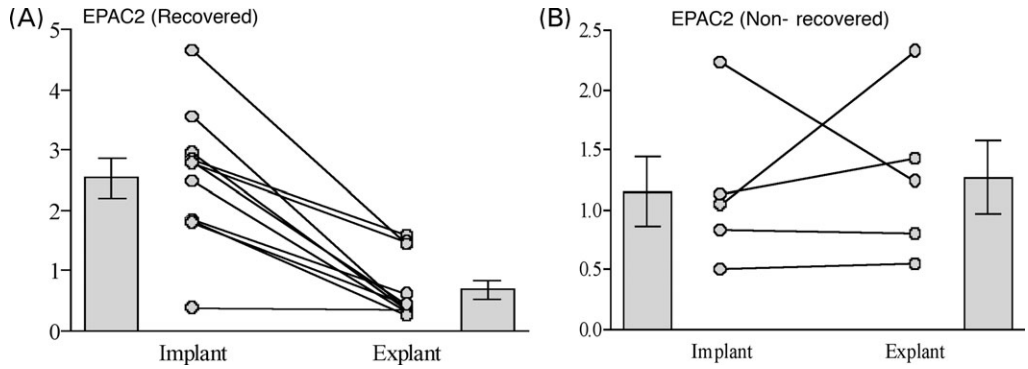

Figure 2 RTQPCR reconfirmed the down-regulation in EPAC2 in the explanted heart samples compared with the paired implant samples in all six recovered patients from the array analysis and extended these findings to an additional five recovered patients, $n = 11$, $P < 0.01$. EPAC2 values were unchanged in a set of non-recovered paired human heart samples ($n = 5$, *P*-value, not significant).

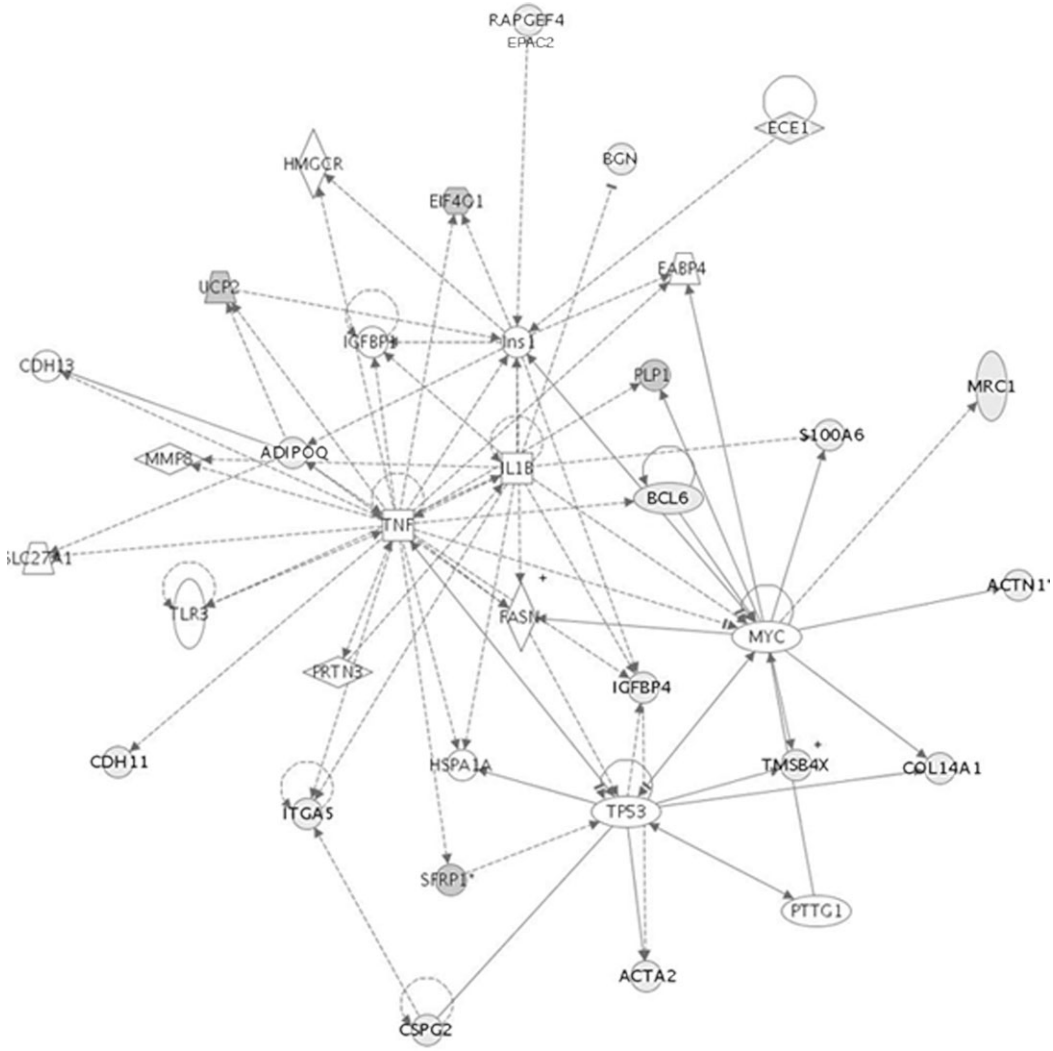

Figure 3 Identification of the potential interactions between genes associated with recovery. Of note is the link between RAPGEF4 (EPAC2) and insulin, and the connection between integrin signalling genes including alpha-5 integrin and alpha-1 actinin with TNF and c-myc, respectively. The fold change in the connected table represents direction in the explanted sample.

Gene symbol	Gene description	Linked to	Entrez ID	Affymetrix	P-value	Fold change
ACTA2	Actin, Alpha 2	TP53	59	200974_at	0.02845	2.6
ACTN1	Actinin, alpha1	MYC	87	208637_x_at	0.009768	2.4
ADIPOQ	adiponectin	TNF/INS1/IL1B	9370	207175_at	0.00491	-4.5
BCL6	B-cell lymphoma 6	MYC	604	203140_at	0.0139	2.2
BCL6	B-cell lymphoma 6	TNF	604	203140_at	0.0139	2.2
BGN	Biglycan	IL1B	633	213905_x_at	0.04486	2.7
CDH11	cadherin 11, type 2	TNF	1009	207173_x_at	0.0295	2.2
COL14A1	collagen, type XIV	MYC/TP53	7373	212865_s_at	0.007741	4.2
CSPG2	versican	TNF/TP53	1462	221731_x_at	0.04835	3.4
ECE1	Endothelin-converting enzyme 1	INS1	1889	201749_at	0.02993	2.2
EIF4G1	eukaryotic translation initiation factor 4 gamma, 1	INS1/TNF	1981	208625_s_at	3.24E–04	1.3
IGFBP4	insulin_like growth factor binding protein 4	INS1/TP53	3487	201508_at	0.03888	2.2
IL1B	interleukin 1, beta	IL1B	3553	205067_at		
Ins1	insulin I	INS1	3630	206598_at		
ITGA5	integrin, alpha 5	TNF/IL1B	3678	201389_at	0.009614	2.0
MRC1	Mannose receptor, C type 1	MYC	4360	204438_at	0.002471	2.1
PLP1	proteolipid protein 1	IL1B/MYC	5354	210198_s_at	0.001075	1.2
RAPGEF4	Rap guanine nucleotide exchange factor (GEF) 4	INS1	11069	205651_x_at	0.044	–2.2
S100A6	S100 calcium binding protein A6 (calcyclin)	IL1B/MYC	6277	217728_at	0.03759	2.7
SFRP1	secreted frizzled-related protein 1	TNF/TP53	6422	202037_s_at	0.00251	–2.0
SLC27A1	solute-carrier family 27	TNF	376497	NA		
TLR3	toll-like receptor 3	TNF	7098	206271_at		
TMSB4X	thymosin, beta 4, X-linked	MYC/TP53	7114	216438_s_at	0.03914	2.1
TNF	tumor necrosis factor (TNF superfamily, member 2)	TNF/MYC/TP53	7124	207113_s_at		
TP53	p53	TP53/MYC/TNF	7157	201746_at		
UCP2	uncoupling protein 2	ADIPOQ/INS1	7351	208998_at	0.02794	1.5

Figure 3 Continued.

ventricular previously function to allow explantation of the device. Given the defined species heterogeneity with respect to β-adrenergic receptor density and signalling,[25] analysis of human tissue provides a significant opportunity to advance our understanding of the regulation and role of adrenergic signalling in human recovery.

EPAC2 has been shown to tether cAMP to MAPK, calcium-mediated signalling through NFAT, and metabolic signalling pathways.[26,27] We reconfirmed the decrease in EPAC2 by RTQPCR (*Figure 2*). Recent work published by our group[28] identified a significant increase in flux through the Kreb's cycle of adult rat cardiac myocytes treated with clenbuterol. In addition, Soppa *et al.*[28] identified a significant improvement in calcium handling in myocytes treated with clenbuterol. It is possible that these affects were in part mediated through EPAC2. The down-regulation in EPAC2 appears to be unique to recovery as we did not find any significant changes in EPAC2 in previously analysed non-recovered samples.

Pathway analysis also identified an integrin pathway that was enriched with genes significantly altered by recovery. This is in agreement with our previous work, demonstrating changes in integrin pathway components (integrins α5, α7, β1, β6, β7, vinculin, α2-actinin, β actin) at both mRNA and protein levels.[19] There is a growing body of evidence that integrins are bidirectional signalling molecules and play a role in mechanotransduction by mediating mechanical (stretch) signals from the extracellular matrix, via protein kinase cascades that provoke changes in gene expression, including those involved in the hypertrophic response.[29–33] These data suggest that the integrin pathway may play a key role at the molecular and cellular level in processes of reverse remodelling and subsequent functional recovery occurring in these patients. Whether patients with ischaemic aetiology would have similar changes in gene expression with this therapy is unclear.

In addition to the finding that the process of recovery was associated with cAMP and integrin signalling, several new targets were identified. Arginine:glycine amidinotransferase (AGAT), a rate-limiting enzyme in the creatine synthesis pathway, was significantly down-regulated following unloading in the recovered hearts, returning to normal levels in direct contrast to the up-regulation of AGAT in patients with heart failure compared with donor hearts.[20] These changes in AGAT mRNA levels suggest a response to heart failure that involves elevated local creatine synthesis. The mechanisms leading to induced AGAT expression are unknown but may be a response to the depletion of the local creatine pool, which we and others have shown to be a feature of heart failure.

We recognize that a sample size of six patients is a limitation of this study. However, the association between genes that are significantly altered in the process of myocardial recovery with the prospective follow-up over a minimal course of 2 years showing ventricular function in all six patients remains normal (mean EF 66%) provides an important starting point. The inclusion of both genders is also a limitation that likely decreases the sensitivity of the analysis. Histological analysis of the pre-LVAD heart samples revealed no sign of acute myocarditis. Furthermore, analysis

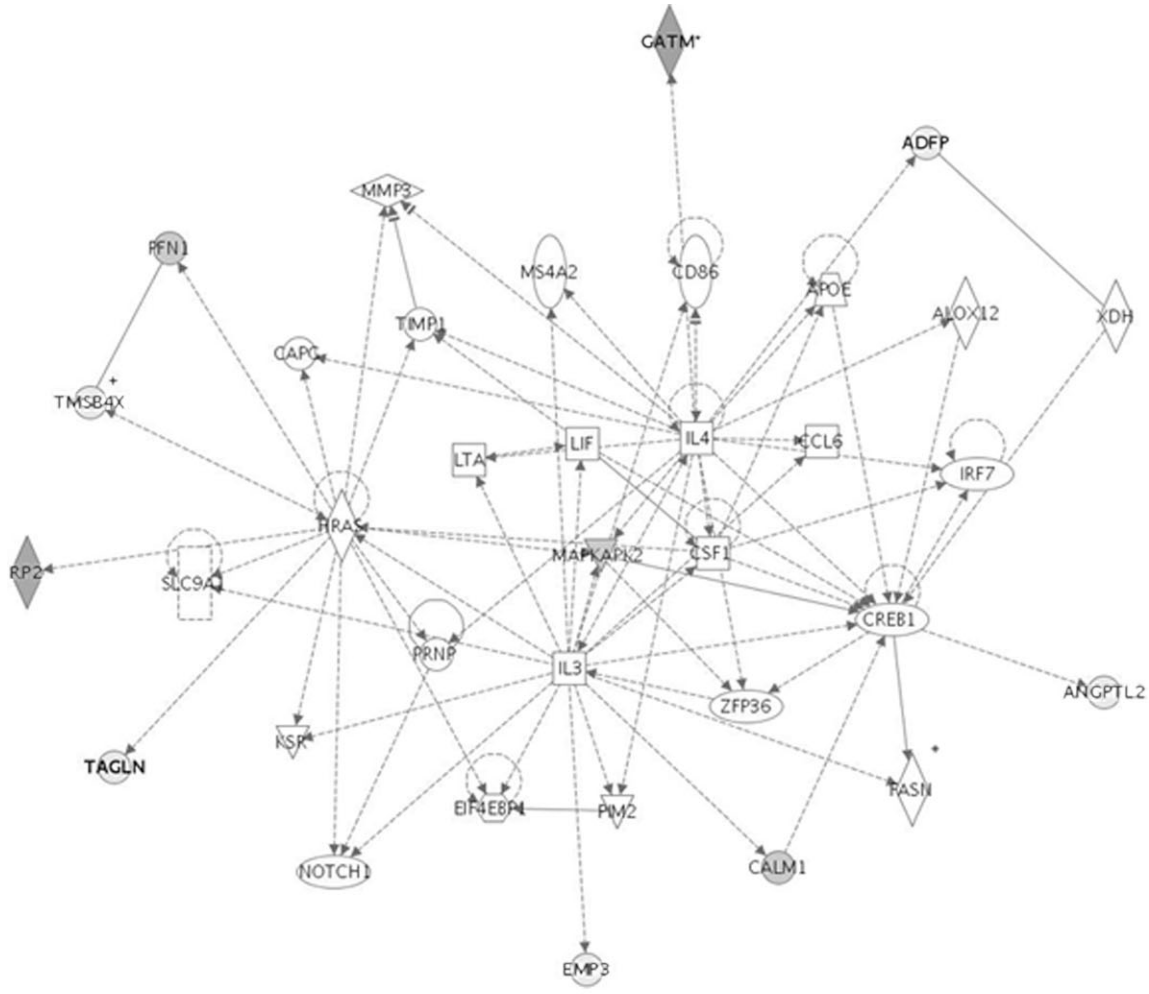

Gene symbol	Gene description	Linked to	Entrez ID	Affymetrix	P-value	Fold change
TAGLN	transgelin	RAS	6876	205547_s_at	0.02461	2.4
ADFP	adipose differentiation-related protein	IL4/XDH	123	209122_at	0.00666	2.0
PFN1	profilin	HRAS	5216	200634_at	0.00414	1.6
RP2	retinitis pigmentosa 2 glycine	HRAS	6102	205191_at	5.17E-04	2.3
GATM	amidinotransferase	IL4	2628	203178_at	4.76E-04	−2.8
IL3	interleukin 3 epithelial membrane	IL3/CREB1	3562	207906_at		
EMP3	protein 3	IL3	2014	203729_at	0.04407	2.1
ANGPTL2	angiopoietin-like 2 harvey rat sarcoma viral	CREB1 HRAS/MA	23452	213001_at	0.01079	2.1
HRAS	ongocgene homolog mitogen-activated protein kinase-activated protein	PKAPK2	3265	212983_at		
MAPKAPK2	kinase 2	RAS/IL4/IL3	9261	201460_at	0.03356	1.2
CREB1	cAMP response element-binding protein 1	MAPKAPK2/IL3	1385	204312_x_at		
CALM1	calmodulin 1 (phosphorylase kinase, delta)	IL3/CREB1	801	213688_at	0.02068	−1.3
TMSB4X	thymosin, beta 4, X-linked	PFN1/FRAS	7114	216438_s_at	0.03914	2.1

Figure 4 Identification of the potential interactions between genes associated with recovery. Note the association of GATM with IL-4. Fold change represents direction in explanted sample.

of the pre-LVAD samples from this recovery cohort with 19 pre-LVAD non-recovered samples in our expression library revealed less than 2% change in the number of statistically significant genes (73 genes) ($P < 0.01$, two-fold change), suggesting our recovered patients are comparable to non-recovered patients prior to LVAD insertion. We are unable to state with certainty that these gene differences are not relevant to the ability to recover. Four of the 73 genes

identified as significantly different between the pre-recovered and the pre-non-recovered were interferon, gamma-inducible protein 16, mannose receptor, C type 1, serine/arginine repetitive matrix 2, and S100 calcium binding protein A10. Despite the relatively small sample size, the paired design of the study helps to alleviate the confounding factor of human heterogeneity. Although the analysis tools used to identify networks and pathways provide an advantageous resource for determining pathways that may be associated with recovery, these programs are currently limited by the amount of information within the database.

In conclusion, this study provides a first molecular signature of clinical recovery in patients with heart failure. This study combines the use of genomics in a unique patient population that represents recovery from end-stage heart failure with follow-up clinical data demonstrating maintained improvement in heart function. Novel associations included a robust regulation of integrin signalling pathways; and a point-specific regulation of a novel gene, EPAC2, in the cAMP signalling pathway that is associated with historical improvements in contractility, β-adrenergic responsiveness, and metabolic signalling. In many ways it is surprising that common pathways and genes are identified that associate with recovery given that the genetic and environmental cues that predisposed these patients to a complex disease such as heart failure are likely to be dissimilar. The use of genome-wide association studies to identify common variants in genes associated with early onset or rapid progression of heart failure in multiple large populations will provide important clues and additional insights in mining microarray datasets such as this. For example, it is foreseeable that we will have the capacity to determine genes whose expression is driven in large part through environmental influences vs. those whose expression is driven in large part by heritable variants in the genome. Incorporating the use of more large-scale platforms and bioinformatics analyses in the study of human heart failure will hopefully advance our understanding of human disease and potentially lead to the identification of new drug therapies to slow or reverse the disease.

Acknowledgements

The authors wish to thank the staff at the University of Minnesota Affymetrix Core Facility, the staff of the Supercomputing Institute for Digital Simulation and Advanced Computation at the University of Minnesota, The Royal Brompton and Harefield Charitable Trustees, Thoratec Corporation, and the British Heart Foundation for their generous support.

Conflict of interest: none declared.

References

1. Jessup M, Brozena S. Heart failure. *N Engl J Med* 2003;**348**:2007–2018.
2. Barton PJ, Birks EJ, Felkin LE, Cullen ME, Koban MU, Yacoub MH. Increased expression of extracellular matrix regulators TIMP1 and MMP1 in deteriorating heart failure. *J Heart Lung Transplant* 2003;**22**:738–744.
3. Barton PJ, Felkin LE, Birks EJ, Cullen ME, Banner NR, Grindle S, Hall JL, Miller LW, Yacoub MH. Myocardial insulin-like growth factor-I gene expression during recovery from heart failure after combined left ventricular assist device and clenbuterol therapy. *Circulation* 2005; **112**:I46–I50.
4. Blaxall BC, Tschannen-Moran BM, Milano CA, Koch WJ. Differential gene expression and genomic patient stratification following left ventricular assist device support. *J Am Coll Cardiol* 2003;**41**:1096–1106.
5. Hall JL, Grindle S, Han X, Fermin D, Park S, Chen Y, Bache RJ, Mariash A, Guan Z, Ormaza S, Thompson J, Graziano J, de Sam Lazaro SE, Pan S, Simari RD, Miller LW. Genomic profiling of the human heart before and after mechanical support with a ventricular assist device reveals alterations in vascular signaling networks. *Physiol Genomics* 2004;**17**:283–291.
6. Huang X, Pan W, Park S, Han X, Miller LW, Hall J. Modeling the relationship between LVAD support time and gene expression changes in the human heart by penalized partial least squares. *Bioinformatics* 2004; **20**:888–894.
7. Margulies KB, Matiwala S, Cornejo C, Olsen H, Craven WA, Bednarik D. Mixed messages: transcription patterns in failing and recovering human myocardium. *Circ Res* 2005;**96**:592–599.
8. Razeghi P, Bruckner BA, Sharma S, Youker KA, Frazier OH, Taegtmeyer H. Mechanical unloading of the failing human heart fails to activate the protein kinase B/Akt/glycogen synthase kinase-3beta survival pathway. *Cardiology* 2003;**100**:17–22.
9. Razeghi P, Young ME, Ying J, Depre C, Uray IP, Kolesar J, Shipley GL, Moravec CS, Davies PJ, Frazier OH, Taegtmeyer H. Downregulation of metabolic gene expression in failing human heart before and after mechanical unloading. *Cardiology* 2002;**97**:203–209.
10. Chen Y, Park S, Li Y, Missov E, Hou M, Han X, Hall JL, Miller LW, Bache RJ. Alterations of gene expression in failing myocardium following left ventricular assist device support. *Physiol Genomics* 2003;**14**:251–260.
11. Rodrigue-Way A, Burkhoff D, Geesaman BJ, Golden S, Xu J, Pollman MJ, Donoghue M, Jeyaseelan R, Houser S, Breitbart RE, Marks A, Acton S. Sarcomeric genes involved in reverse remodeling of the heart during left ventricular assist device support. *J Heart Lung Transplant* 2005; **24**:73–80.
12. Chaudhary KW, Rossman EI, Piacentino V III, Kenessey A, Weber C, Gaughan JP, Ojamaa K, Klein I, Bers DM, Houser SR, Margulies KB. Altered myocardial Ca2+ cycling after left ventricular assist device support in the failing human heart. *J Am Coll Cardiol* 2004;**44**:837–845.
13. Chen X, Piacentino V III, Furukawa S, Goldman B, Margulies KB, Houser SR. L-type Ca2+ channel density and regulation are altered in failing human ventricular myocytes and recover after support with mechanical assist devices. *Circ Res* 2002;**91**:517–524.
14. Harding JD, Piacentino V III, Gaughan JP, Houser SR, Margulies KB. Electrophysiological alterations after mechanical circulatory support in patients with advanced cardiac failure. *Circulation* 2001;**104**:1241–1247.
15. Rose EA, Gelijns AC, Moskowitz AJ, Heitjan DF, Stevenson LW, Dembitsky W, Long JW, Ascheim DD, Tierney AR, Levitan RG, Watson JT, Meier P, Ronan NS, Shapiro PA, Lazar RM, Miller LW, Gupta L, Frazier OH, Desvigne-Nickens P, Oz MC, Poirier VL. Long-term mechanical left ventricular assistance for end-stage heart failure. *N Engl J Med* 2001;**345**:1435–1443.
16. Birks EJ, Tansley PD, Yacoub MH, Bowles CT, Hipkin M, Hardy J, Banner NR, Khaghani A. Incidence and clinical management of life-threatening left ventricular assist device failure. *J Heart Lung Transplant* 2004;**23**:964–969.
17. Yacoub MH, Tansley P, Birks EJ, Banner NR, Khaghani A, Bowles C. A novel combination therapy to reverse end-stage heart failure. *Transplant Proc* 2001;**33**:2762–2764.
18. Birks EJ, Tansley P, Hardy J, RS G, Bowles C, M B, Banner NR, A K, Yacoub MH. Reversal of severe heart failure with left ventricular assist and pharmacologic therapy. *N Engl J Med* 2006;**355**:1873–1884.
19. Birks EJ, Hall JL, Barton PJ, Grindle S, Latif N, Hardy JP, Rider JE, Banner NR, Khaghani A, Miller LW, Yacoub MH. Gene profiling changes in cytoskeletal proteins during clinical recovery after left ventricular-assist device support. *Circulation* 2005;**112**:I57–I64.
20. Cullen ME, Yuen AH, Felkin LE, Smolenski R, Hall JL, Grindle S, Miller LW, Birks EJ, Yacoub MH, Barton PJ. Myocardial expression of the arginine: glycine aminotransferase gene is elevated in heart failure and normalized following post-LVAD recovery: potential implications for local creatine synthesis. *Circulation* (accepted, Scientific Sessions, American Heart Association Meetings, 2005)
21. Aquila LA, McCarthy PM, Smedira NG, Young JB, Moravec CS. Cytoskeletal structure and recovery in single human cardiac myocytes. *J Heart Lung Transplant* 2004;**23**:954–963.

22. Dipla K, Mattiello JA, Jeevanandam V, Houser SR, Margulies KB. Myocyte recovery after mechanical circulatory support in humans with end-stage heart failure. *Circulation* 1998;**97**:2316–2322.
23. Ogletree-Hughes ML, Stull LB, Sweet WE, Smedira NG, McCarthy PM, Moravec CS. Mechanical unloading restores beta-adrenergic responsiveness and reverses receptor downregulation in the failing human heart. *Circulation* 2001;**104**:881–886.
24. Terracciano CM, Harding SE, Adamson D, Koban M, Tansley P, Birks EJ, Barton PJ, Yacoub MH. Changes in sarcolemmal Ca entry and sarcoplasmic reticulum Ca content in ventricular myocytes from patients with end-stage heart failure following myocardial recovery after combined pharmacological and ventricular assist device therapy. *Eur Heart J* 2003;**24**:1329–1339.
25. Rockman HA, Koch WJ, Lefkowitz RJ. Seven-transmembrane-spanning receptors and heart function. *Nature* 2002;**415**:206–212.
26. Holz GG. Epac: a new cAMP-binding protein in support of glucagon-like peptide-1 receptor-mediated signal transduction in the pancreatic beta-cell. *Diabetes* 2004;**53**:5–13.
27. Seino S, Shibasaki T. PKA-dependent and PKA-independent pathways for cAMP-regulated exocytosis. *Physiol Rev* 2005;**85**:1303–1342.
28. Soppa GK, Smolenski RT, Latif N, Yuen AH, Malik A, Karbowska J, Kochan Z, Terracciano CM, Yacoub MH. Effects of chronic administration of clenbuterol on function and metabolism of adult rat cardiac muscle. *Am J Physiol Heart Circ Physiol* 2005;**288**:H1468–H1476.
29. Barberis L, Wary KK, Fiucci G, Liu F, Hirsch E, Brancaccio M, Altruda F, Tarone G, Giancotti FG. Distinct roles of the adaptor protein Shc and focal adhesion kinase in integrin signaling to ERK. *J Biol Chem* 2000; **275**:36532–36540.
30. Brancaccio M, Fratta L, Notte A, Hirsch E, Poulet R, Guazzone S, De Acetis M, Vecchione C, Marino G, Altruda F, Silengo L, Tarone G, Lembo G. Melusin, a muscle-specific integrin beta1-interacting protein, is required to prevent cardiac failure in response to chronic pressure overload. *Nat Med* 2003;**9**:68–75.
31. Brancaccio M, Hirsch E, Notte A, Selvetella G, Lembo G, Tarone G. Integrin signalling: the tug-of-war in heart hypertrophy. *Cardiovasc Res* 2006;**70**:422–433.
32. De Acetis M, Notte A, Accornero F, Selvetella G, Brancaccio M, Vecchione C, Sbroggio M, Collino F, Pacchioni B, Lanfranchi G, Aretini A, Ferretti R, Maffei A, Altruda F, Silengo L, Tarone G, Lembo G. Cardiac overexpression of melusin protects from dilated cardiomyopathy due to long-standing pressure overload. *Circ Res* 2005;**96**:1087–1094.
33. Keller RS, Shai SY, Babbitt CJ, Pham CG, Solaro RJ, Valencik ML, Loftus JC, Ross RS. Disruption of integrin function in the murine myocardium leads to perinatal lethality, fibrosis, and abnormal cardiac performance. *Am J Pathol* 2001;**158**:1079–1090.